

FUZZY LOGIC CONTROLLER FOR DEPTH CONTROL OF UNDERWATER REMOTELY OPERATED VEHICLE

¹MOHD SHAHRIEEL MOHD ARAS, ²SHAHRUM SHAH ABDULLAH, ³SITI YASMIN BINTI OTHMAN, ⁴MARIZAN SULAIMAN, ⁴MOHD FARRIZ BASAR, ⁵MOHD KHAIRI MOHD ZAMBRI, ⁶MUHAMMAD NIZAM KAMARUDIN

¹Asstt Prof., Department of Mechatronics, Faculty of Electrical Engineering, Universiti Teknikal Malaysia Melaka, MALAYSIA

²Assoc. Prof., Department of Electrical and Electronics Engineering, Malaysia-Japan International Institute of Technology, Kuala Lumpur, MALAYSIA

³Student, Department of Mechatronics, Faculty of Electrical Engineering, Universiti Teknikal Malaysia Melaka, MALAYSIA

⁴Prof., Department of Power Systems, Faculty of Electrical Engineering, Universiti Teknikal Malaysia Melaka, MALAYSIA

⁵Asstt Prof., Department of Electrical Engineering, Faculty of Technology Engineering, Universiti Teknikal Malaysia Melaka, MALAYSIA

⁶Lecturer, Department of Mechatronics, Faculty of Electrical Engineering, Universiti Teknikal Malaysia Melaka, MALAYSIA

⁷Asstt Prof., Department of Mechatronics, Faculty of Electrical Engineering, Universiti Teknikal Malaysia Melaka, MALAYSIA

E-mail: ¹shahrieel@utem.edu.my

ABSTRACT

Nowadays, unmanned underwater vehicle (UUV) is created to reduce human intervention in deep-water application. UUV can help human to make an underwater application that commonly used in deep water industries. During operation, the UUV undergoes a complex multi-axis motion trajectories that are highly nonlinear because the subsystems in the UUV are ill-defined and strongly coupled to each other. The conventional controller such as Proportional, Integral and Derivative (PID) and Proportional and Derivative (PD) have a problem to control nonlinear operation. The conventional controller hardly to achieve zero overshoot. Implementation of the controller on the UUV using Fuzzy Logic Controller (FLC) itself poses its own level of complexity. Consequently, implementation of FLC also requires fast and high-performance processors. The objectives of this paper are to study the effect of the tuning membership function to improved performances of the FLC for depth control using actual underwater Remotely Operated Vehicle (ROV) based on VideoRay ROV Pro III as well as to analyze performance of system response of depth control in terms of zero overshoot, faster rise time and small steady state error. Then, the proposed approach is verified using hardware interfacing between MATLAB/Simulink and Microbox 2000/2000C. The result shows FLC gives rather best performance in term of faster rise time, zero overshoot and small steady state error as compared with conventional controllers.

Keywords: *Fuzzy Logic Controller; Depth Control; Remotely operated Vehicle; Tuning Membership Function*

1. INTRODUCTION

Underwater Remotely Operated Vehicle (ROV) commonly used in deep water industries which is involved in oil and gas activities. ROVs are widely used in offshore construction, military and scientific community. The ROV is used to replace the manned rescue system in military and helps scientist in a research on underwater knowledge,

deep sea animal and plants. The project focuses on designing the Fuzzy Logic Controller (FLC) in order to improve the transient response such as minimum overshoot, faster rise time, small steady state error for depth control of the ROV. The main objectives of this project to improve the performances of the FLC for depth control because the ROVs is widely used in several underwater applications. ROV also can be used to explore

science or natural environment at the seabed. Paper [1] mentioned about impacts of using ROV which is the two hundred ninety individuals completed the questionnaire in 2005. Mysterious tragedy for MH370 also used the ROV in searching black box in a seabed of the Southern Indian Ocean. The ROV can firm, scan and crucially pick up things from the seabed as shown in Figure 1. Another example is Remora which can function 6000 metres which is used in salvage AF447 and other crashed planes [2].

The important thing in the ROV is the control system. However, the scope of this project is only concerned with the dynamics in the vertical motion considered in the depth control approach. In order to enhance a better control design for depth control, the analysis from FLC is introduced in this paper.



Figure 1: ROV Helps Missing MH370 [2]

There are many problems happen with the ROV that related to control system discussed in [3-5]. The control system of an ROV is an interesting and challenging problem. This is primarily due to the difficult and unpredictable environmental conditions that exist underwater [6]. During operation, the ROV undergoes a complex multi-axis motion trajectories that are highly nonlinear because the subsystems in the ROV are ill-defined and strongly coupled with one another [7]. Furthermore, the ROV dynamics perturbed considerably by the surrounding conditions and external disturbances (e.g. wind velocity, ocean currents and waves) [8].

The conventional controller such as PD also has a problem with depth control of the ROV. The PD controller is not suitable for nonlinear operation of depth control. Also, the conventional PID controller also hardly to achieve zero overshoot in system response of depth control [8]. For vertical trajectory, overshoot in the system response will be one of the factors to be measured because overshoot is particularly dangerous in the ROV

vertical trajectory and may cause damage to both the ROV and the inspected structure (e.g. operating in cluttered environments). Thus, an intelligent control such as FLC is needed in order to improve performances of the system. In this approach, a shifting membership function in the input membership function of FLC will be used to analyze the effect of system response of depth control. The results show a simple contribution to this field of study.

To reach main result and objective, the prototype ROV based on actual ROV VideoRay Pro III was built. The prototype of the ROV is built by following parameters of thruster configuration of ROV VideoRay Pro III (2 horizontal thruster and 1 vertical thruster). The dimension of prototypes built up by referring to VideoRay Pro 3s (30.5 x 22.5 x 21cm). Since this project related with depth control, the movement of ROV covered a vertical movement. The depth of ROV while doing an experiment is set less than 5m only. This project was carried out under the assumption of zero disturbance (controlled environment). This project were interfacing with Microbox 2000/2000C for the real time experiment.

2. LITERATURE REVIEW

According to Aras et al. [9], system identification is used in developing the model of the ROV for depth control. The system identification concept is a process of obtaining model based on a set of data that collected from open loop experiments. Firstly, the ROV is tested in open loop condition in order to get input and output signal value which is using 5m as a set point for depth control. The recorded value from input and output was analyzed to infer a model as shown in Figure 2. Then, system identification toolbox in MATLAB will be applied to generate models of the ROV. This research also compares the mathematical modelling and system identification. The result shows a mathematical modelling better than system identification as shown in Figure 3. However, system identification more towards in term of real time applications which is included environmental disturbances in lab tank test or in a swimming pool [9].

According to M.S.M Aras [10], the investigation of linear approximation control surface method for tuning single input fuzzy logic controller (SIFLC) is focused on the slope of linear equations as shown in Figure 3. Firstly, the

optimum operating conditions are determined in order to generalize the output equation of linear surface. The derivation of output equations of linear surface, it shows that the control surface shape is determined by the peak location of the input and output of membership functions. Lastly, examples of different linear approximation and its original relationship to FLC will be described. In this journal, the best slope of linear equations is 0.5 as shown in Figure 5 where gives better performances than others. If the slope bigger, the response of system is not good and chattering happen. In depth control, the chattering must be eliminated in order to avoid damage to the ROV [10].

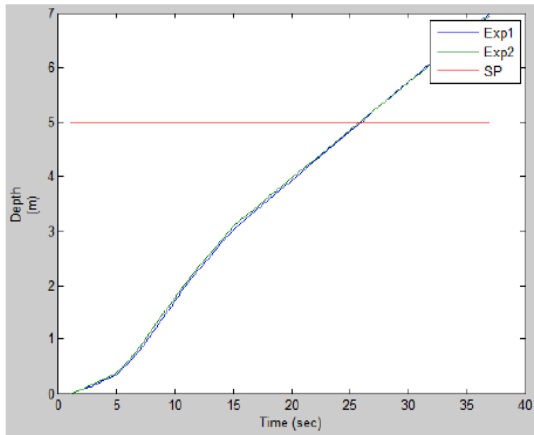


Figure 2: Experiment Results Testing Open Loop System For ROV [2]

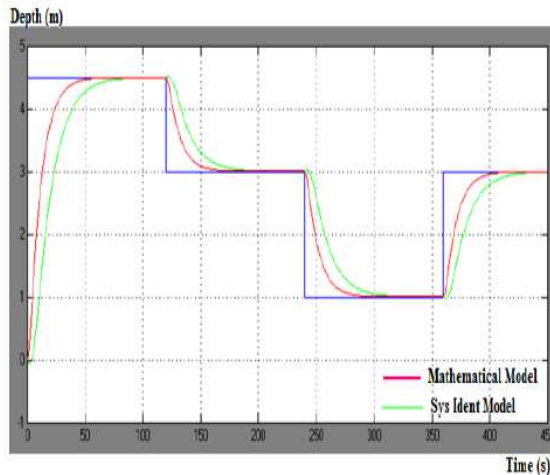


Figure 3: Comparison Between Mathematical Models With System Identification Model [9]

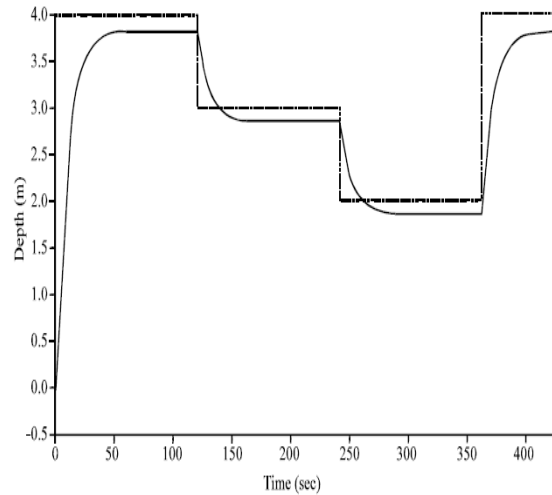


Figure 4: The System Response Of ROV System Based On Linear Equation [10]

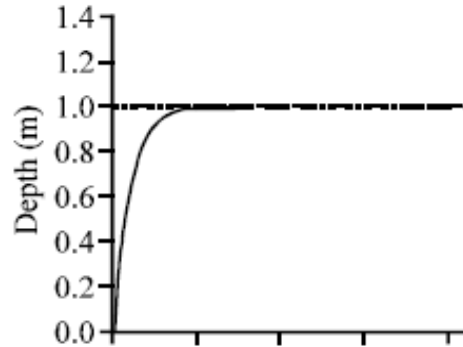


Figure 5: Slope Of 0.5 Linear Equation [10]

Table 1: Comparison Between Conventional Controller And Intelligent Controller

Controller	Advantages	Disadvantages
Single input fuzzy logic controller (SIFLC) [3]	Slope of linear equation give optimum performances	Different control surface of piecewise linear region effect performance of depth control
PD controller [4]	Able to reduce overshoot. Suitable for larger gain by adding damping to the system	Not suitable for non-linear operation.
PID Controller with disturbance occurrence [5]	Easy to implement	Changing parameters effect times of regulation prolongation
Fuzzy Logic Controller [1][3][4][5]	Suitable for non-linear operation and able to apply heuristic rules that reflect experiences of the human experts.	Fine tuning process is highly time consuming.

3. METHODOLOGY

For the first phase, the literature review regarding existing method control system for depth control of the ROV as shown in Table 1. Next, the

simulation process to analyze performance of system response for depth control by using MATLAB/ Simulink. Then, the prototype of VideoRay Pro III was built, so that the analysis system response in real time with Microbox 2000/2000C were covered. The effect of system response by shifting output membership function of fuzzy logic controller also included in this project.

The Prototype (VideoRay Pro III Underwater Vehicle)

The prototype based on VideoRay Pro III underwater vehicle are used in this project. VideoRay Pro III is a small inspection class personal as shown in Figure 7. The vehicle has three control thrusters, one for vertical movement and two for horizontal movement. It is designed for depth control of 152 meters deep. The vehicle includes sensor, front and rear facing camera, depth gauge and heading meter. Mapping thruster based on this underwater vehicle will be implemented in this project, as shown in Figure 8 (a) and 8 (b).

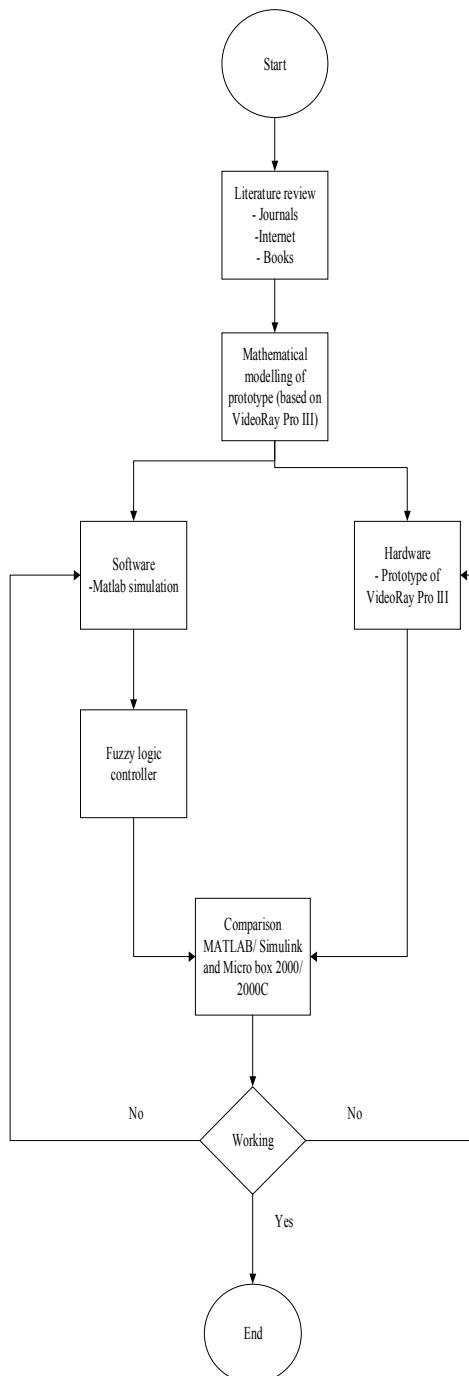
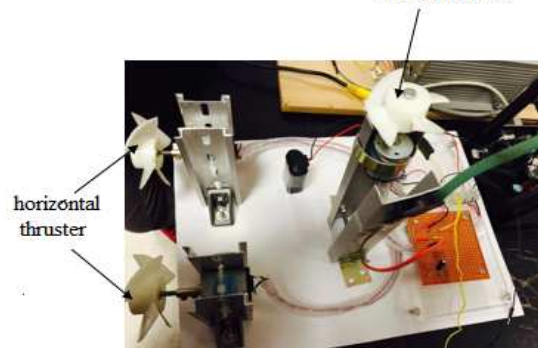


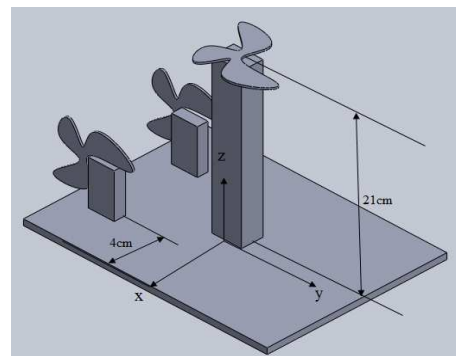
Figure 6: Flow Chart Of Methodology



Figure 7: Videoray Pro III Underwater Vehicle Prototype Based On Videoray Pro III



(a)



(b)

Figure 8: Thruster Configuration Based On Videoray Pro III

Mathematical Modelling

For mathematical modelling, all parameters are based on properties and the coefficients of ROV VideoRay Pro III data on [11-13] into a matrix using Newton-Euler motion equation. The generated equation will import to workspace in MATLAB. Then, the mathematical modelling of ROV will be controlled using conventional PID controller. Mathematical modelling is derived from the Newton-Euler motion equation 1 [14-15].

$$M\dot{v} + C(v) + D(v)v + G = T \tag{1}$$

The mathematical modelling was derived as shown equation (2 – 5). The value of a matrix based on properties and coefficient of VideoRay Pro III [11]. The mass, $m= 43\text{kg}$ follows a mass of VideoRay Pro III. The value of -16.24 implies that the vehicle has residual buoyancy. The residual buoyancy equates to 4% of the vehicle’s weight.

$$M_{RB} = \begin{pmatrix} m & 0 & 0 & 0 & 0 & 0 \\ 0 & m & 0 & 0 & 0 & 0 \\ 0 & 0 & m & 0 & 0 & 0 \\ 0 & 0 & 0 & I_x & 0 & 0 \\ 0 & 0 & 0 & 0 & I_y & 0 \\ 0 & 0 & 0 & 0 & 0 & I_z \end{pmatrix} \tag{2}$$

$$M_A = \begin{pmatrix} X\dot{u} & 0 & 0 & 0 & 0 & 0 \\ 0 & 0 & 0 & 0 & 0 & 0 \\ 0 & 0 & Z\dot{w} & 0 & 0 & 0 \\ 0 & 0 & 0 & 0 & 0 & 0 \\ 0 & 0 & 0 & 0 & 0 & 0 \\ 0 & 0 & 0 & 0 & 0 & N\dot{r} \end{pmatrix} \tag{3}$$

$$D(v) = \begin{pmatrix} X & 0 & 0 & 0 & 0 & 0 \\ 0 & 0 & 0 & 0 & 0 & 0 \\ 0 & 0 & Y & 0 & 0 & 0 \\ 0 & 0 & 0 & 0 & 0 & 0 \\ 0 & 0 & 0 & 0 & 0 & 0 \\ 0 & 0 & 0 & 0 & 0 & Z \end{pmatrix} \tag{4}$$

$$G = \begin{pmatrix} 0 \\ 0 \\ B - W \\ 0 \\ 0 \\ 0 \end{pmatrix} \tag{5}$$

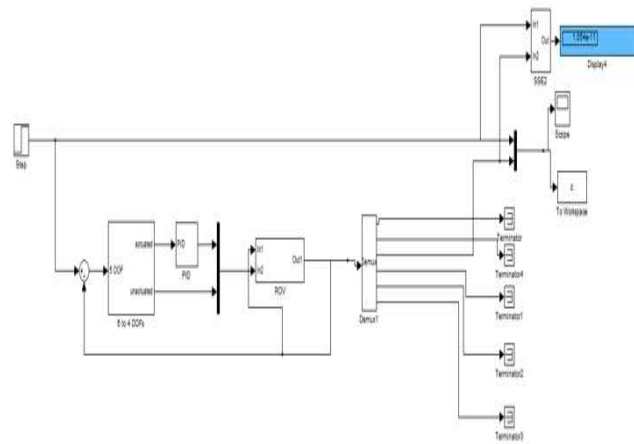


Figure 9: Simulation Of ROV Modelling

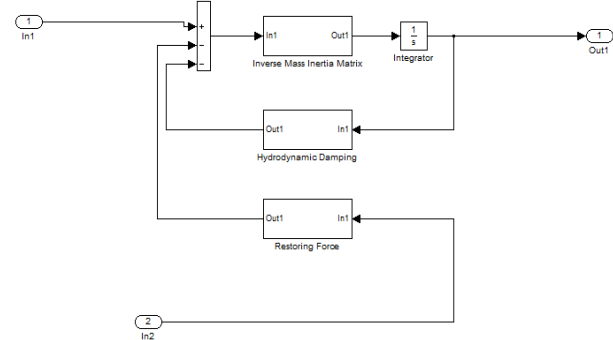


Figure 10: Subsystem Of The Mathematical Modelling Of The ROV

Fuzzy Logic Controller using MATLAB/ Simulink

MATLAB software are used to create an FLC based on fuzzy logic toolbox as shown in Figure 11. The rules editor used to construct a rule statement of the fuzzy logic as shown in Table 2. Figure 13 shows the rule viewer of rules and Figure 14 shows the surface of rules in 3D. In order to design a closed loop FLC, the pressure sensor experiment needs to be performed and able to obtain real-time data. The data obtained will be evaluated by the system identification toolbox. Then, system identification are used to infer a

model. Model obtained then implemented in closed-loop FLC system as shown in Figure 15.

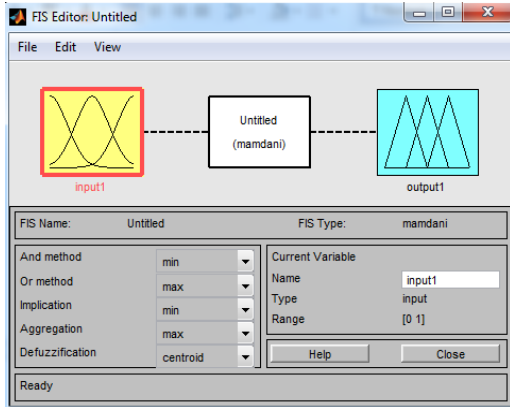


Figure 11: Fis Editor

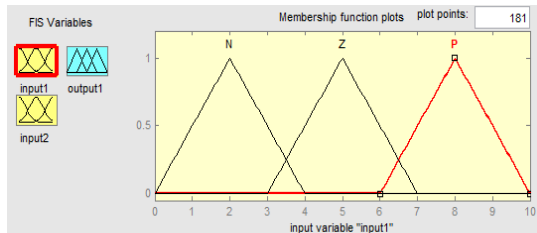


Figure 12: Input 1 Membership Function

Table 2: Rule table for fuzzy logic

IP 1 \ IP 2	N	Z	P
N	N	Z	P
Z	N	Z	P
P	N	Z	P

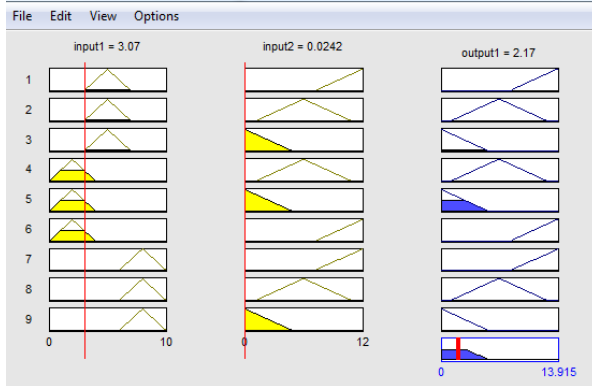


Figure 13: Rules Viewer Of Fuzzy Logic Controller

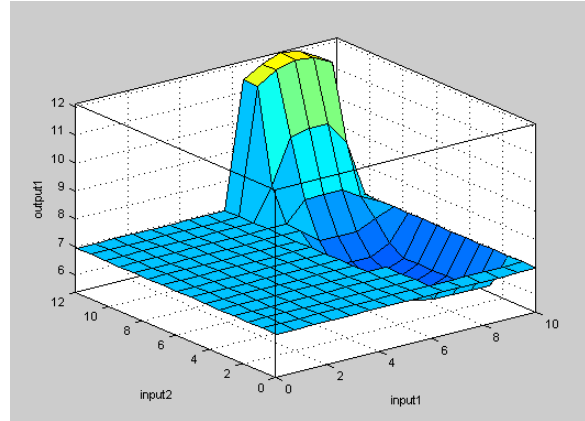


Figure 14: Rules Surface Of Fuzzy Logic Controller

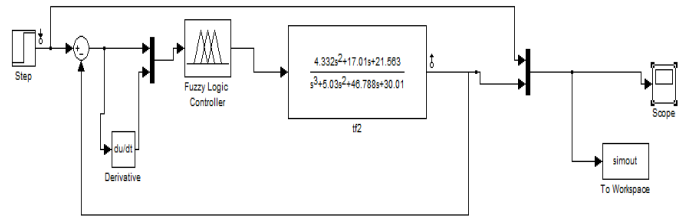


Figure 15: Simulation Real-Time Of Fuzzy Logic Controller

A Real-Time Simulation System using Microbox 2000/2000c

After the experiment, the several data were analyzed by system identification technique. The best data was chosen to use to infer a model of the ROV. Then, implemented in MATLAB/Simulink to study the performance of system response using PID and fuzzy logic controller. The experiment was set up using Microbox 2000/2000c, prototype (based on VideoRay Pro III), pressure sensor circuit, mini compressor, and multimeter.

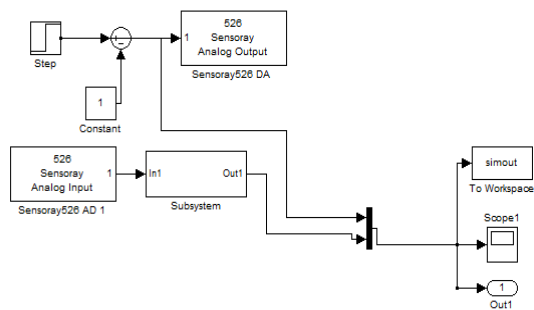


Figure 16: Real Time Open Loop System

4. RESULTS AND DISCUSSION

Table 3: Output Response Of Mathematical Modelling

Table 3 shows the output performance in terms of rise time, settling time, overshoot and steady state error for the mathematical modelling approach. The result shows no overshoot, faster rise time, and small steady state error achieved. The output response of mathematical modelling based on VideoRay Pro III as shown in Figure 17. Since the roll, pitch and sway were considered negligible; then, the M_{RB} can be simplified to a good approximation Equation (2) –(5) which further simplified to Equation (6) – (9).

Type of control system	Tr (s)	Ts (s)	Overshoot (%)	Steady state error
Mathematical modelling (PID)	2.1407	5.5639	0	0

$$M_{RB} = \begin{pmatrix} 43 & 0 & 0 & 0 & 0 & 0 \\ 0 & 0 & 0 & 0 & 0 & 0 \\ 0 & 0 & 43 & 0 & 0 & 0 \\ 0 & 0 & 0 & 0 & 0 & 0 \\ 0 & 0 & 0 & 0 & 0 & 0 \\ 0 & 0 & 0 & 0 & 0 & 0.02532 \end{pmatrix} \quad (6)$$

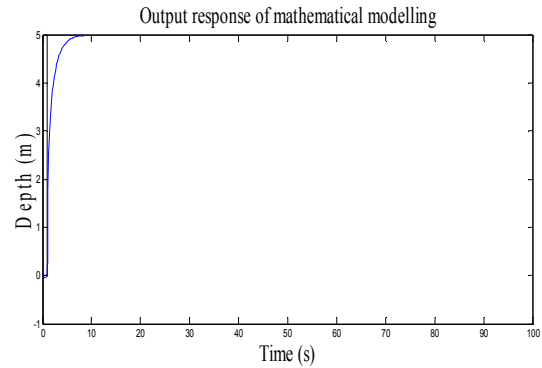


Figure 17: Graph Output Response Of Mathematical Modelling

$$M_A = \begin{pmatrix} 1.9404 & 0 & 0 & 0 & 0 & 0 \\ 0 & 0 & 0 & 0 & 0 & 0 \\ 0 & 0 & 3.9482 & 0 & 0 & 0 \\ 0 & 0 & 0 & 0 & 0 & 0 \\ 0 & 0 & 0 & 0 & 0 & 0 \\ 0 & 0 & 0 & 0 & 0 & 0.0321 \end{pmatrix} \quad (7)$$

$$D(v) = \begin{pmatrix} 10.586 & 0 & 0 & 0 & 0 & 0 \\ 0 & 0 & 0 & 0 & 0 & 0 \\ 0 & 0 & 26.3392 & 0 & 0 & 0 \\ 0 & 0 & 0 & 0 & 0 & 0 \\ 0 & 0 & 0 & 0 & 0 & 0 \\ 0 & 0 & 0 & 0 & 0 & 0.0137 \end{pmatrix} \quad (8)$$

$$G = \begin{pmatrix} 0 \\ 0 \\ -16.24 \\ 0 \\ 0 \\ 0 \end{pmatrix} \quad (9)$$

Table 4 shows the system performance of real time data in term of rise time, settling time, overshoot and steady state error. Several real time data were tested and verified by using system identification. In Table 4, a data 11 shows the best performance in terms on no overshoot, faster rise time, settling time and small steady state error value. The transfer function of data 11 was chosen as model for PID and fuzzy logic controller.

Table 5 shows an output response of real-time simulation PID controller before tuning process. The result of the rise time, settling time, overshoot and steady state error become increase than real-time open loop simulation result. The automatic tuning process was applied to the simulation system in order to get a better performance. Table 6 shows a result after 4 times applied tuning process. When times of tuning process are increased, the percentage of overshoot display a better value, but the rise time and settling time shows an increment value while steady state error remains the same. Table 7 shows the simulation result of automatic tuning PID parameter.

Effect of membership function for real-time Fuzzy Logic Controller

Table 8 shows the result of change range of input 1 of fuzzy logic. The result shows when range input 1 was increased, the output response display unchanged condition (not applicable). Table 9 shows the result by changing range input 2

of fuzzy logic while the range input 1 set of 0-10. The output response displays unchanged condition same as the output response in Table 8. Table 10 shows the output response of fuzzy logic simulation by changing range of output. The condition of output response change when output ranges from 0-14. In this range the fastest rise time, and small steady state error able to obtain while zero overshoot condition was not achieved. When the range change to 0-13.91, the zero overshoot condition able to achieve while rise time and settling time value was increased. The steady state error value remains same.

Based on result in Table 10, changing the range of the output membership function of FLC will affect the output response. The input 1 and input 2 range value were not affected the performance of the fuzzy logic controller system. The experiment continues by shifting membership function of fuzzy logic to increase the output performance. Table 11 shows the output performance in terms of average rise time and settling time. In Table 11, the input 1 was shifted to the center, left and right. The faster average rise time and settling time indicate the better performance. The shifting input 1 to the 'center' display the better value than 'left' and 'right'. Table 12 shows the output response (overshoot and steady state error) by shifting input 1 in three conditions. Output response displays the same value although, in different shifting condition.

The summary of average output performance for input 1 was tabulated in Table 13. The change of each performance was calculated in order to evaluate the best shifting membership function. The 'center' condition shows the same performance. The 'left' condition displays decreased performance in terms of rise time and settling time. The 'right' condition remains the same performance except settling time shows a decreasing performance. In Table 14, the shifting membership function input 1 on 'center condition' shows the better performance than other condition. Average output performance of rise time and settling by shifting membership function input 2 as shown in Table 15. The best rise time and settling time when input 2 in 'right' shifting condition. Table 16 shows the average percentage overshoot and steady state error input 2 which remains same in all shifting conditions.

Table 17 indicates the summary of average output performance for shifting membership

function input 2. The comparison between three shifting condition as shown in Table 18. 'Center' shifting conditions remains the same performance. The 'left' condition displays decreasing performance in terms of rise time. The increasing performance shows in settling time. The overshoot and steady state error remain same performance at 'center' condition. The overshoot, steady state error and rise time of 'center' condition shows same performance while settling time obtained the better performance. Average output performance of rise time and settling time by shifting membership function output as shown in Table 19. The best rise time and settling time when output in 'right' shifting condition than 'center' and 'left'. Overshoot and steady state value for 'left' and 'right' remains same while 'center' in not applicable condition as shown in Table 20.

The change of each output performance in three different shifting conditions as shown in Table 21. The performance was evaluated between 'left' and 'right' shifting condition. When the output shifting to the 'center', the rise time, settling time, percentage overshoot and steady state error remains same performance. When the output shifting to the 'right' the settling time shows increasing performance while other parameter indicate the same performance as shown in Table 22. Table 23 shows a results for shifting membership function input 1, input2, and output. In Table 24, the same performance of 'center' and 'right' for rise time. The 'left' condition shows a decreasing performance. The settling time of 'left' shows increasing performance, but 'right' condition shows decreasing performance, while 'center' remains same performance. The zero overshoot were achieved by shifting membership function of the 'center' and 'right' only. The steady state error at 'left' condition shows increasing performance than 'center' and 'right'.

Based on Table 25, it shows the best result output performance of fuzzy logic controller in experiment 8 that involves three shifting conditions. Table 26, it clearly shows the output performance of rise time, settling time, overshoot and steady state error with different type of controller. The fuzzy logic controller shows the fast rise time and settling time than mathematical modelling and PID. All types of control achieved no overshoot condition. The mathematical modelling show the small steady state error than PID and fuzzy logic controller. The output



response from different type of controller as shown in Table 27.

5. CONCLUSION

As a conclusion, the experiment shows that using PID controller, a zero overshoot performance condition is achieved. However the value of rise time is increased. Then, experiment on FLC was used as a control system in order to achieve a better output performance. Based on result, it clearly shows a fuzzy logic controller display a better performance, which is 0.75s faster rise time than PID and 0.60 differences in term of steady state error. The output performance of FLC in term of faster rise time, zero overshoot and small steady state error were better than PID. The mathematical modelling of the ROV is used by using properties and a coefficient of VideoRay Pro III. The output response of model simulation shows a smooth shape of the graph. The zero overshoot with faster rise time and the small steady state error was achieved. The pressure sensor that used as a feedback in the control system. The analog to digital converter able to construct by using pressure sensor data. The zero overshoot was able to achieve by using real-time PID simulation, but the performance of rise time and settling time were decreased. The steady state error maintains at 1. The data 11 was chosen to implement into a fuzzy logic controller. All real-time data shown observable and controllable result. However, the data 1 shown asymptotic unstable. The experiment was conducted to study the effect of real time fuzzy logic controller. Result show that the fuzzy logic controller display the best response for faster rise time and settling time. The zero overshoot and small steady state error also achieved.

ACKNOWLEDGEMENT

We wish to express our gratitude to honorable University, Universiti Teknikal Malaysia Melaka (UTeM) and Universiti Teknologi Malaysia (UTM). Special appreciation and gratitude to especially for Underwater Technology Research Group (UTeRG), Centre of Research and Innovation Management (CRIM), Ministry of Higher Education for supporting this research under FRGS (FRGS/1/2015/TK04/FKE/02/F00257) and to both Faculty of Electrical Engineering from UTeM and UTM.

REFERENCES

- [1] California State University, Northridge. "Fluid Pressure," www.csun.edu [Online]. Available: www.csun.edu/science/activities/pressure/fluid-pressure [Accessed: November 28, 2014].
- [2] CNN. "Behind The Scenes: Filming Remotely Operated Underwater Vehicles at Sea," edition.cnn.com. [Online]. Available:edition.cnn.com/2014/04/01/world/europe/scotland-rov-demonstration [Accessed: Oct 1, 2014].
- [3] S. M. Zanoli and G. Conte, "Remotely operated vehicle depth control," Control Eng. Pr., vol. 11, no. 4, pp. 453–459, 2003.
- [4] Mohd Aras, Mohd Shahrieel and Abdul Rahman, Ahmad Fadzli Nizam (2013) Analysis of an Improved Single Input Fuzzy Logic Controller Designed For Depth Control Using Microbox 2000/2000c Interfacing. International Review of Automatic Control, 6 (6). pp. 728-733. ISSN 1974-6059
- [5] Mohd Aras, Mohd Shahrieel and Ab Rashid, Mohd Zamzuri and Azhan , Ab. Rahman (2013) Development And Modeling Of Unmanned Underwater Remotely Operated Vehicle Using System Identification For Depth Control. Journal of Theoretical and Applied Information Technology, Vol 56 (1). pp. 136-145. ISSN 1992-8645
- [6] Hou, C. S. The effects of the umbilical cable and current on the motion of the underwater remotely operated vehicle. Master thesis. National Cheng University. China. 2005.
- [7] A. M. Plotnik and S. M. Rock. A multi-sensor approach to automatic tracking of midwater targets by an ROV. Proceedings of the American Institute of Aeronautics and Astronautics (AIAA), 2007.
- [8] Louis Andrew Gonzalez. Design, Modelling and Control of an Autonomous Underwater Vehicle. Master Thesis. University of Western Australia. 2007.
- [9] Aras M.SM, Abdullah S.S and Rashid M.Z.A, "Development and Modelling Of Unmanned Underwater Remotely Operated Vehicle Using System Identification for Depth Control" Theoretical and Applied Information Technology, 2013, Vol. 56. No.1.
- [10] Aras M.SM, Abdullah S.S and Rashid M.Z.A, "Tuning Process of Single Input Fuzzy Logic Controller Based on Linear Control Surface Approximation Method for Depth Control of Underwater Remotely Operated Vehicle" Engineering and Applied Sciences, 208-214,2013.
- [11] Wei Wang and Christopher M. Clark, "Modelling and Simulation of the VideoRay Pro III Underwater Vehicle" University of Waterloo, Canada, 208-214, 2012.
- [12] Russell B. Wynn, Veerle A.I. Huvenne, Timothy P. Le Bas, Bramley J. Murton, Douglas P. Connelly,



- Brian J. Bett, Henry A. Ruhl, Kirsty J. Morris, Jeffrey Peakall, Daniel R. Parsons, Esther J. Sumner, Stephen E. Darby, Robert M. Dorrell, James E. Hunt, Autonomous Underwater Vehicles (AUVs): Their past, present and future contributions to the advancement of marine geoscience, *Marine Geology*, Volume 352, 1 June 2014, Pages 451-468
- [13] Vega, E., Chocron, O., Benbouzid, M., AUV Propulsion Systems Modeling Analysis, (2014) *International Review on Modelling and Simulations (IREMOS)*, 7(5), pp. 827-837. doi:<http://dx.doi.org/10.15866/iremos.v7i5.3648>
- [14] Jebelli, A., Yagoub, M., Rahim, R., Kazemi, H., Design and Construction of an Underwater Robot Based Fuzzy Logic Controller, (2013) *International Review of Mechanical Engineering (IREME)*, 7(1), pp. 147-153.
- [15] Mashhad, A., Karsaz, A., Mashhadi, S., High Maneuvering Multiple-Underwater Robot Tracking with Optimal Two-Stage Kalman Filter and Competitive Hopfield Neural Network Based Data Fusion, (2013) *International Journal on Communications Antenna and Propagation (IRECAP)*, 3(4), pp. 191-198.

Table 4: System performance of real time data

Data	Rise Time (Tr)	Settling Time (Ts)	Overshoot (%)	Steady state
1	296	452	0	-38.3
2	2.58	75.4	13	1.22e03
3	0.00471	5.99	2.72e03	0.115
4	256	453	0	34
10	1.9	36.1	57.4	-6.81e04
11	0.202	4.94	0	0.719

Table 5: Output response of real-time simulation PID controller

Real time result	Tr	Ts	Overshoot (%)	Ess
	6.94s	11.1s	0.275	1

Table 6: Result of automatic tuning PID

Tuning process	Rise Time(s)	Settling Time(s)	Overshoot (%)	Steady state error
1	6.94	11.1	0.275	1
2	9.02	15.5	0.0000	1
3	12.3	22.1	0	1
4	10.3	18	0	1

Table 7: Simulation result of automatic tuning PID

Tuning process	Tr	Diff. Tr	Ts	Diff. Ts	%OS	Diff. %OS	Ess	Diff. Ess
1	6.94	NA	11.1	NA	0.275	NA	1	NA
2	9.02	-2.080	15.5	-4.4000	0.00002	0.2749	1	0
3	12.3	-5.3600	22.1	-11.00	0	0.2750	1	0
4	10.3	-3.3600	18	-6.9	0	0.2750	1	0

Table 8: Simulation result for change range input 1

Range	Tr	Diff. Tr	Ts	Diff. Ts	%OS	Diff. %OS	Settling max	Ess	Diff. Es
0-2	NA	NA	NA	NA	0	0	NA	NA	NA
0-4	NA	NA	NA	NA	0	0	NA	NA	NA
0-6	NA	NA	NA	NA	0	0	NA	NA	NA
0-8	NA	NA	NA	NA	0	0	NA	NA	NA
0-10	NA	NA	NA	NA	0	0	NA	NA	NA

Table 9: Simulation result for change range input 2

Range	Tr	Diff. Tr	Ts	Diff. Ts	%OS	Diff. %OS	Settling max	Ess	Diff. Es
0-2	NA	NA	NA	NA	0	0	NA	NA	NA
0-4	NA	NA	NA	NA	0	0	NA	NA	NA
0-6	NA	NA	NA	NA	0	0	NA	NA	NA
0-8	NA	NA	NA	NA	0	0	NA	NA	NA
0-10	NA	NA	NA	NA	0	0	NA	NA	NA



Table 10: Simulation result for change range output

Range	Tr	Diff. Tr	Ts	Diff. Ts	%OS	Diff. %OS	Max Settling	Ess	Diff. Es
0-2	NA	NA	NA	NA	0	0	NA	NA	NA
0-4	NA	NA	NA	NA	0	0	NA	NA	NA
0-6	NA	NA	NA	NA	0	0	NA	NA	NA
0-8	NA	NA	NA	NA	0	0	NA	NA	NA
0-10	NA	NA	NA	NA	0	0	NA	NA	NA
0-12	NA	NA	NA	NA	0	0	NA	NA	NA
0-14	0.199	NA	4.5633	NA	0.2016	0	4.9974	0.9974	NA
0-13.91	0.2016	-0.0026	4.9741	-0.4108	0	0.2016	4.9974	0.9974	0

Table 11: Average rise time and settling time for input 1 membership function

Shifting condition	Tr				Ts			
	1	2	2	Average	1	2	3	Average
Center	0.2015	0.2015	0.2015	0.2015	4.9482	4.9481	4.9481	4.9481
Left	0.2029	0.2009	0.2013	0.2017	4.9685	4.9739	4.9685	4.9664
Right	0.2015	0.2015	0.2015	0.2015	4.9483	4.9481	4.9481	4.9482

Table 12: Average percent overshoot and steady state error of input 1

Shifting condition	Overshoot (%)				Max Settling				Ess
	1	2	2	Average	1	2	3	Average	Average
Center	0	0	0	0	4.9992	4.9992	4.9992	4.9992	0.99
Left	0	0	0	0	4.9979	4.9974	4.9979	4.9977	0.99
Right	0	0	0	0	4.9992	4.9992	4.9992	4.9992	0.99

Table 13: Summary of average output performance for input 1

Shifting condition	Tr	Diff. Tr	Ts	Diff. Ts	%OS	Diff. %OS	Max. Settling	Ess	Diff. Ess
Center	0.2015	NA	4.9481	NA	0	NA	4.9992	0.99	NA
Left	0.2017	-0.0002	4.9664	-0.0183	0	0	4.9977	0.99	0
Right	0.2015	0	4.9482	-0.0002	0	0	4.9992	0.99	0

Table 14: Simulation performance of input 1 membership function

Shifting condition	Tr	Ts	%OS	Ess
Center	Same performance	Same performance	Same performance	Same performance
Left	Decreasing performance	Decreasing performance	Decreasing performance	Decreasing performance
Right	Same performance	Decreasing performance	Same performance	Same performance

Legend

- Same performance
- Increasing performance
- Decreasing performance

Table 15: Average rise time and settling time of input 2 membership function

Shifting condition	Tr				Ts			
	1	2	2	Average	1	2	3	Average
Center	0.2015	0.2015	0.2015	0.2015	4.9482	4.9481	4.9481	4.9482
Left	0.2046	0.2015	0.2015	0.2025	4.9481	4.9481	4.9481	4.9481
Right	0.2015	0.2015	0.2015	0.2015	4.9481	4.9481	4.9481	4.9481



Table 16: Average rise time and settling time of input 2 membership function

Shifting condition	Overshoot (%)				Max Settling				Ess Average
	1	2	2	Average	1	2	3	Average	
Center	0	0	0	0	4.9992	4.9992	4.9992	4.9992	0.99
Left	0	0	0	0	4.9992	4.9992	4.9992	4.9992	0.99
Right	0	0	0	0	4.9992	4.9992	4.9992	4.9992	0.99

Table 17: Summary of average output performance for input 2

Shifting condition	Tr	Diff. Tr	Ts	Diff. Ts	%OS	Diff. %OS	Max. Settling	Ess	Diff. Ess
Center	0.2015	NA	4.9482	NA	0	NA	4.9992	0.99	NA
Left	0.2025	-0.001	4.9481	0.0001	0	0	4.9992	0.99	0
Right	0.2015	0	4.9481	0.0001	0	0	4.9992	0.99	0

Table 18: Simulation performance of input 2 membership function

Shifting condition	Tr	Ts	%OS	Ess
Center	Yellow	Yellow	Yellow	Yellow
Left	Red	Green	Yellow	Yellow
Right	Yellow	Green	Yellow	Yellow

Legend

- Same performance
- Increasing performance
- Decreasing performance

Table 19: Average rise time and settling time of output membership function

Shifting condition	Tr				Ts			
	1	2	2	Average	1	2	3	Average
Center	0.2015	0.2015	NA	NA	4.9554	5.8813	NA	NA
Left	0.2015	0.2015	0.2015	0.2015	4.9253	4.9493	9.2299	6.3682
Right	0.2015	0.2015	0.2015	0.2015	4.9664	4.9560	4.8574	4.9266

Table 20: Average overshoot and steady state error of output membership function

Shifting condition	Overshoot (%)				Max Settling				Ess Average
	1	2	2	Average	1	2	3	Average	
Center	0	0	NA	NA	4.9992	4.9992	NA	NA	NA
Left	0	0	0	0	4.9992	4.9992	4.9992	4.9992	0.99
Right	0	0	0	0	4.9992	4.9992	4.9992	4.9992	0.99

Table 21: Summary of average output performance for output

Shifting condition	Tr	Diff. Tr	Ts	Diff. Ts	%OS	Diff. %OS	Max. Settling	Ess	Diff. Ess
Center	NA	NA	NA	NA	NA	NA	NA	NA	NA
Left	0.2015	NA	6.3682	NA	0	NA	4.9992	0.99	NA
Right	0.2015	0	4.9481	1.4201	0	0	4.9992	0.99	0

Table 22: Simulation performance of output membership function

Shifting condition	Tr	Ts	%OS	Ess
Center	Yellow	Yellow	Yellow	Yellow
Left	Yellow	Yellow	Yellow	Yellow
Right	Yellow	Green	Yellow	Yellow

Legend

- Same performance
- Increasing performance
- Decreasing performance



Table 23: Simulation result for shifting membership function

Shifting condition	Tr	Diff. Tr	Ts	Diff. Ts	%OS	Diff. %OS	Max. Settling	Ess	Diff. Ess
Center	0.2015	NA	4.9481	NA	0	NA	4.9992	0.99	NA
Left	0.2045	-0.003	3.4590	1.4891	1.6347	-1.6347	5.0817	0.08	0.91
Right	0.2015	0	4.9483	-0.0002	0	1.6347	4.9992	0.99	0

Table 24: Simulation performance for shifting of membership function

Shifting condition	Tr	Ts	%OS	Ess
Center	Yellow	Yellow	Yellow	Yellow
Left	Red	Green	Red	Green
Right	Yellow	Red	Yellow	Yellow

Legend

Yellow	Same performance
Green	Increasing performance
Red	Decreasing performance

Table 25: Summary result for effect of shifting membership function

Shifting condition	Tr	Diff. Tr	Ts	Diff. Ts	%OS	Diff. %OS	Ess	Diff. Ess
Input 1 (Center)	0.2015	NA	4.9481	NA	0	NA	0.99	NA
Input 2 (Right)	0.2015	0	4.9481	0	0	0	0.99	0
Output (Right)	0.2015	0	4.9481	0	0	0	0.99	0
Input 1, Input 2, Output (Center)	0.2015	0	4.9481	0	0	0	0.99	0

Table 26: Summary of output response for each membership function

Membership function	Tr(s)	Ts(s)	%OS	Ess
Input 1 'center'	0.2015	4.9481	0	0.99
Input 2 'right'	0.2015	4.9481	0	0.99
Output 'right'	0.2015	4.9481	0	0.99
Input 1, input 2, output 'center'	0.2015	4.9481	0	0.99

Table 27: Comparison output response with different type of controller

Type of controller	Rise time (s)	Settling time (s)	Overshoot (%)	Steady state error
Mathematical modelling	2.1407	5.5639	0	0
Real time PID	10.3	18	0	1
Real time of fuzzy logic controller	0.2015	4.9481	0	0.99